

SYNTHESIS, CHARACTERIZATION, AND PHOTOCATALYTIC PROPERTIES OF WO₃/TiO₂ NANOCOMPOSITES VIA GREEN SYNTHESIS METHODS USING LEMONGRASS EXTRACT

Tanzeela Faiz¹, Tahira Bibi², Delawar Ashraf³, Ramzan Ullah⁴, Huma Arif⁵, Asadullah Talib⁶, Muqddas Hameed⁷, Durr Muhammad^{*8}

¹Department of Physics, NFC Institute of Engineering and Technology, Multan, Pakistan.

²Department of Botany, Sardar Bahadur Khan Women's University, Quetta, Pakistan.

³Department of Chemistry, University of Florida, America.

⁴School of Chemical Engineering, Tianjin University, China.

⁵Department of Chemistry, University of Poonch Rawalakot Azad Kashmir, Pakistan.

⁶Department of Physics, The Islamia University of Bahawalpur, Bahawalnagar Campus, Pakistan.

⁷Department of Chemistry, University of Sahiwal, Sahiwal, Pakistan.

⁸North University of China, Taiyuan, Shanxi Province, China

¹tanzeelaifaiz128@gmail.com, ²tahira_botany@yahoo.com, ³ashraf.delawar@ufl.edu,

⁴engramzan@tju.edu.cn, ⁵humaarif.3333@gmail.com, ⁶asadshaib9@gmail.com,

⁷muqddashameed1214@gmail.com, ⁸durmuhammad@yahoo.com

DOI: <https://doi.org/10.5281/zenodo.15834286>

Keywords

Green synthesis, Photocatalysis, TiO₂, WO₃, Nanocomposites, Lemongrass extract.

Article History

Received on 28 May 2025

Accepted on 28 June 2025

Published on 07 July 2025

Copyright @Author

Corresponding Author: *

Durr Muhammad

Abstract

This research presents a green synthesis route for pure TiO₂, WO₃, and TiO₂/WO₃ nanocomposites using lemongrass (*Cymbopogon flexuosus*) extract as a natural reducing and stabilizing agent. Characterization techniques such as SEM, EDX, FTIR, XRD, and UV-Vis spectroscopy confirmed the morphology, purity, structural integrity, and optical properties of the materials. Band gap energies were found to be 3.01 eV (TiO₂), 2.92 eV (WO₃), 2.81 eV (TiO₂/WO₃ 2:1), and 2.49 eV (TiO₂/WO₃ 1:1). Photocatalytic efficiency was evaluated by degrading methylene blue (MB) under solar light. The 1:1 TiO₂/WO₃ composite demonstrated superior degradation performance. This study supports the application of green-synthesized nanocomposites in environmental remediation.

INTRODUCTION

Nanotechnology deals with materials ranging from 1 to 100 nanometers and includes particles with unique properties compared to their bulk counterparts. Among metal oxides, TiO₂ and WO₃ stand out due to their photocatalytic activity, chemical stability, and environmental relevance. TiO₂ has a wide band gap

and high oxidative potential but suffers from limited solar utilization. WO₃, with a narrower band gap, offers better visible-light activity. Combining these semiconductors enhances photocatalytic properties through better charge separation and extended absorption range.

Green synthesis methods using plant extracts like lemongrass provide a sustainable alternative to conventional synthesis, avoiding toxic chemicals while introducing bioactive molecules that aid in nanoparticle stabilization. Lemongrass extract contains phytochemicals like citral and geraniol that serve as reducing agents.

This study aims to synthesize TiO_2 , WO_3 , and TiO_2/WO_3 nanocomposites via green methods, characterize those using advanced analytical tools, and evaluate their photocatalytic activity against MB dye under solar irradiation.

Nanoscience and nanotechnology have emerged as transformative fields, greatly influencing various branches of science and technology over the last few decades. The term "nano", where materials that exhibit unique mechanical, optical, magnetic, and electrical properties distinct from their bulk counterparts (Eychmüller, 2000; Edelstein & Cammarata, 1998). Nanotechnology has significantly impacted sectors such as electronics, energy storage, environmental purification, and biomedical applications (Sim & Wong, 2021; Zhou et al., 2011). As research continues to expand, the production and characterization of nanomaterials remain critical for technological advancement.

Nanoparticles (NPs) are a major class of nanomaterials categorized based on their chemical composition into organic and inorganic types (Kiyamov et al., 2020; Khan et al., 2019). Organic nanoparticles include lipid bodies, proteins, and nanoclusters, while inorganic nanoparticles typically consist of metal and metal oxide particles such as ZnO , CuO , and TiO_2 (Jeon & Baek, 2010; Siddiqui et al., 2020). The remarkable properties of nanoparticles – such as large surface area, quantum confinement effects, and reactivity – make them suitable for applications in imaging, catalysis, drug delivery, and energy devices (Saleh & Elkord, 2020; Gong et al., 2021).

Among various metal oxides, Titanium Dioxide (TiO_2) is extensively studied due to its chemical stability, strong oxidative properties, and biocompatibility (Fujishima et al., 2000; X. Chen & Mao, 2007). TiO_2 primarily exists in three crystalline forms: anatase, rutile, and brookite, with anatase being widely used for photocatalytic applications because of its higher photoactivity (Nosaka & Nosaka, 2016). Despite these advantages, TiO_2 has a wide

band gap (~ 3.2 eV) that limits its absorption to the ultraviolet (UV) range, thus reducing its overall photocatalytic efficiency under solar light (Kalathil et al., 2013).

To overcome the limitations of TiO_2 , it is often combined with other semiconductors such as Tungsten Trioxide (WO_3). WO_3 is an n-type semiconductor with a smaller bandgap (~ 2.5 – 2.8 eV), allowing it to absorb visible light more efficiently (Hariharan et al., 2019; Sánchez Martínez et al., 2011). The incorporation of WO_3 with TiO_2 can enhance light absorption, promote better charge separation, and reduce recombination rates of photogenerated electron-hole pairs, resulting in improved photocatalytic performance (Salje et al., 1997; Han et al., 2021).

Green synthesis methods have gained immense popularity for producing nanoparticles in an eco-friendly, cost-effective, and sustainable manner. Biological methods, using plant extracts, offer a clean route by acting as natural reducing and stabilizing agents (Nguyen et al., 2018; Parveen et al., 2016). Plants like lemongrass (*Cymbopogon flexuosus*) are particularly valuable due to their rich phytochemical content – including citral, geraniol, and citronella – which facilitate nanoparticle formation without the need for hazardous chemicals (Srivastava, 2022).

Water pollution caused by organic dyes and contaminants poses a severe environmental threat, necessitating efficient water purification technologies (Sahoo & Goswami, 2024). Photocatalysis using metal oxide nanocomposites such as TiO_2/WO_3 is a promising approach for degrading organic pollutants and disinfecting water (Goutam et al., 2020). Combining the properties of TiO_2 and WO_3 in a nanocomposite structure could leverage their complementary properties for effective photocatalytic activity under solar irradiation.

Thus, this research aims to synthesize Pure TiO_2 , Pure WO_3 , and TiO_2/WO_3 nanocomposites via a green method using lemongrass extract, characterize the synthesized materials using advanced techniques (SEM, EDX, FTIR, XRD, UV-Vis), and evaluate their photocatalytic efficiency for the degradation of methylene blue dye under solar irradiation.

I. Study Model

This study follows a systematic green synthesis and characterization approach for developing TiO_2 , WO_3 , and $\text{TiO}_2\text{-WO}_3$ nanocomposites. Initially, **plant extract preparation** was performed using lemongrass leaves to provide a natural reducing and stabilizing agent. The **synthesis** of individual nanoparticles (TiO_2 , WO_3) and their nanocomposites ($\text{TiO}_2\text{-WO}_3$) was conducted through a green method, followed by a **calcination** step to enhance crystallinity and structural stability.

The synthesized materials underwent **comprehensive characterization** using XRD (for crystal structure

analysis), SEM (for surface morphology), FTIR (for functional group identification), and UV-Vis spectroscopy (for optical property evaluation). Their photocatalytic efficiency was subsequently assessed through **MB dye degradation** under solar irradiation. Finally, an **efficiency comparison** was performed to identify the material with superior photocatalytic performance.

This model design ensures an eco-friendly synthesis route, thorough material evaluation, and practical performance analysis relevant for environmental applications.

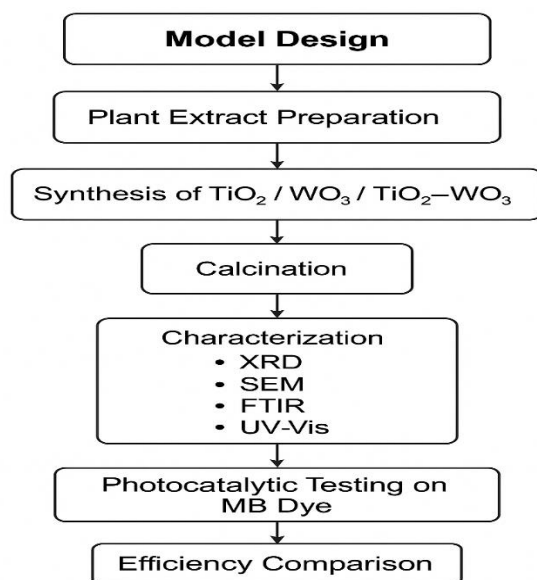


Fig. 1 Block Diagram Study Model

III. Methodology

Materials and Reagents

All chemicals used in this study, including titanium (IV) oxide (TiO_2) and tungsten (VI) oxide (WO_3) precursors, were of analytical grade and employed without further purification. Fresh lemongrass (*Cymbopogon flexuosus*) leaves were procured locally and used as a natural reducing and stabilizing agent in the green synthesis process. Deionized water was used in all experimental procedures to maintain high purity standards and prevent contamination.

2. Preparation of Plant Extract

Fresh lemongrass (*Cymbopogon flexuosus*) leaves were thoroughly rinsed with deionized water to

eliminate surface contaminants and subsequently air-dried at ambient temperature. Approximately 50 grams of the dried leaves were finely ground using a mortar and pestle to obtain a uniform paste. The resulting paste was boiled in 200 mL of deionized water for 30 minutes at a controlled temperature of 70–80°C to extract the phytochemicals. After cooling to room temperature, the mixture was filtered through Whatman No. 1 filter paper, and the resulting extract was stored at 4°C for subsequent use as a natural reducing and stabilizing agent in the nanoparticle synthesis process.

3. Green Synthesis of TiO₂ Nanoparticles

TiO₂ nanoparticles were synthesized via a green route using lemongrass extract as a bio-reducing agent. Specifically, 50 mL of the prepared extract was added to a 0.5 M solution of the titanium precursor under constant magnetic stirring. The reaction mixture was maintained at 80°C for 2 hours to promote the reduction of metal ions and the nucleation of nanoparticles. Upon completion, the resulting precipitate was separated by centrifugation at 6000 rpm for 10 minutes, followed by successive washing with deionized water and ethanol to remove unreacted species and organic residues. The purified product was then dried at 100°C overnight and subsequently calcined at 500°C for 3 hours to improve crystallinity and phase purity.

4. Green Synthesis of WO₃ Nanoparticles

WO₃ nanoparticles were synthesized using a similar green synthesis protocol as applied for TiO₂. Specifically, 50 mL of lemongrass extract was introduced into a 0.5 M aqueous solution of the tungsten precursor under vigorous magnetic stirring. To facilitate the precipitation process and adjust the pH, hydrochloric acid was added dropwise. The reaction mixture was maintained at 80°C for 2 hours to enable the reduction and nucleation of WO₃ nanoparticles. The resulting precipitate was then isolated by centrifugation, thoroughly washed with deionized water and ethanol, and dried at 100°C overnight. The dried powder was subsequently calcined at 500°C for 3 hours to enhance crystallinity and ensure phase purity.

5. Synthesis of TiO₂/WO₃ Nanocomposites

TiO₂/WO₃ nanocomposites were synthesized by combining TiO₂ and WO₃ in molar ratios of 1:1 and 2:1. The respective quantities of the synthesized metal oxide powders were dispersed in deionized water, followed by the addition of lemongrass extract to facilitate green-mediated composite formation. The resulting suspension was continuously stirred at 80°C for 3 hours to ensure homogenous mixing and promote interfacial interactions. After the reaction, the precipitate was collected by centrifugation, thoroughly washed with deionized water and ethanol, and dried at 100°C overnight. The dried composite powder was subsequently calcined at

500°C for 3 hours to enhance crystallinity and strengthen the interfacial bonding between the two metal oxides.

6. Characterization Techniques

A range of advanced techniques was employed to characterize the synthesized nanoparticles and nanocomposites:

- **X-ray Diffraction (XRD)**
Used to determine the crystalline structure, phase composition, and average crystallite size. Data were collected over a 2θ range of 10°–80° using Cu K α radiation ($\lambda = 1.5406 \text{ \AA}$).

- **Scanning Electron Microscopy (SEM) and Energy Dispersive X-ray Spectroscopy (EDX):**
SEM analysis provided detailed insights into surface morphology and particle size, while EDX confirmed the elemental composition and the absence of impurities.

- **Fourier Transform Infrared Spectroscopy (FTIR):**
FTIR spectra were recorded in the range of 400–4000 cm⁻¹ to identify the functional groups and confirm successful synthesis.

- **Ultraviolet-Visible (UV-Vis) Spectroscopy:**
Optical absorption properties and band gap energies were evaluated using UV-Vis spectroscopy. Tauc plots were constructed to estimate the optical band gaps of TiO₂, WO₃, and the TiO₂/WO₃ nanocomposites.

7. Evaluation of Photocatalytic Activity

The photocatalytic performance was assessed by monitoring the degradation of methylene blue (MB) dye under solar irradiation. For each test, 0.05 g of the photocatalyst was dispersed in 100 mL of a 10 ppm MB solution. Before irradiation, the solution was stirred in the dark for 30 minutes to achieve adsorption–desorption equilibrium. The suspension was then exposed to direct sunlight, and aliquots were collected at regular intervals (every 30 minutes). The samples were centrifuged to remove catalysts, and the concentration of MB was measured spectrophotometrically at 664 nm.

The photocatalytic degradation efficiency (%) was calculated using the formula:

$$\text{Degradation Efficiency} = \left(\frac{C_0 - C_t}{C_0} \right) \times 100$$

Where C_0 Is the initial concentration and C_t Is the concentration at time t ?

Results and Discussion

1. Scanning Electron Microscopy (SEM) Analysis

Scanning Electron Microscopy (SEM) was employed to investigate the surface morphology and particle size distribution of the synthesized nanomaterials. SEM provides high-resolution surface images, offering detailed insights into the size, structure, and homogeneity of nanoparticles (Zhou, 2007). To enhance conductivity and imaging quality, a thin layer of gold was sputter-coated onto the samples under vacuum conditions.

The SEM image of titanium dioxide (TiO_2) nanoparticles (Figure 4.1) revealed a homogeneous

distribution of spherical particles with smooth surfaces, with particle sizes predominantly ranging between 45–55 nm and an average diameter of 49 nm. These findings are consistent with previous studies, indicating effective control over synthesis parameters. For tungsten trioxide (WO_3) nanoparticles (Figure 4.2), an oval morphology with an average particle size of 49 nm was observed at 500 nm magnification.

Additionally, SEM images of TiO_2/WO_3 nanocomposites at molar ratios of 1:1 and 2:1 (Figures 4.3 and 4.4) also displayed an oval morphology, with an average particle size of approximately 44 nm. The uniform particle size distribution across all samples highlights the success of the green synthesis method, which is critical for enhancing the photocatalytic efficiency of the materials.

Figure 4.2: SEM images of pure WO_3 NPs at

Figure 4.1: SEM images of pure TiO_2 NPs at $0.5\mu\text{m}$ with 30,000 resolution.

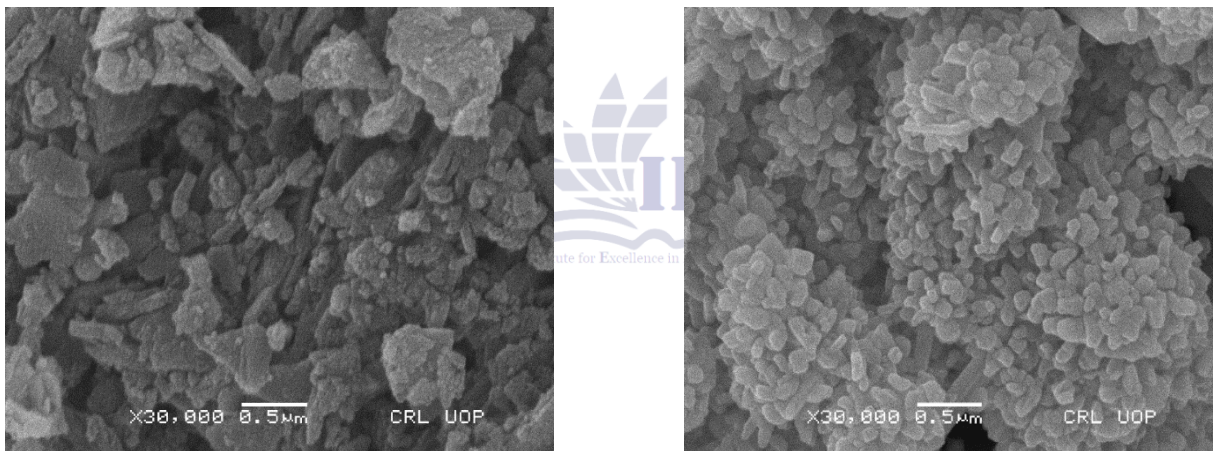
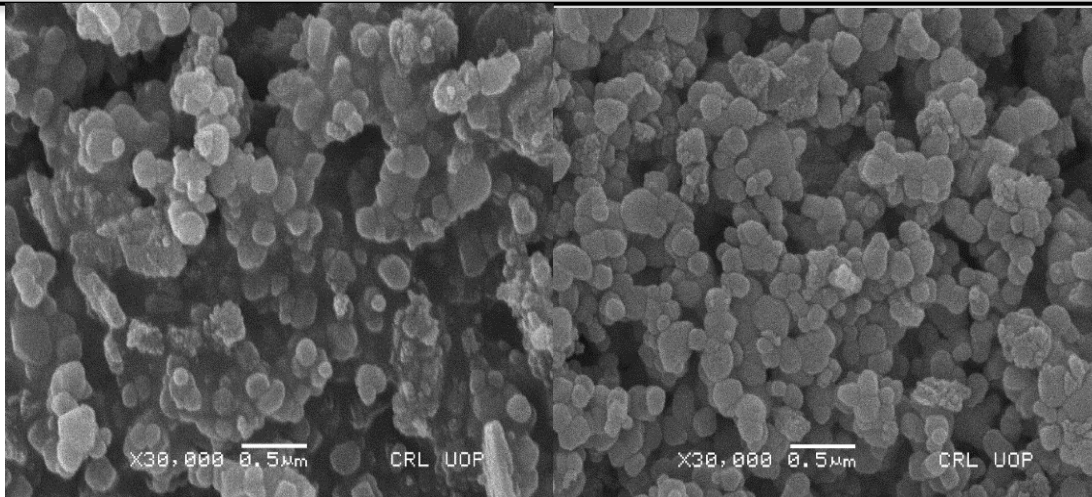


Figure 4.3: SEM images of TiO_2/WO_3 (1:1) at $0.5\mu\text{m}$ with 30,000 resolution



2. Energy Dispersive X-ray Spectroscopy (EDX)

Energy Dispersive X-ray Spectroscopy (EDX), operated in conjunction with Scanning Electron Microscopy (SEM), was utilized to determine the elemental composition of the synthesized samples. EDX detects characteristic X-rays emitted from a material upon electron beam bombardment, allowing qualitative and quantitative elemental analysis. In the EDX spectrum (Figure 4.7) for titanium dioxide (TiO_2), distinct peaks at approximately 4.51 keV ($\text{K}\alpha$) and 4.93 keV ($\text{K}\beta$) confirmed the presence of titanium, while a peak near 0.52 keV corresponded to oxygen, indicating TiO_2 formation. Similarly, the EDX spectrum of tungsten trioxide (WO_3) (Figure 4.8) showed peaks at 8.39 keV ($\text{L}\alpha$), 9.67 keV ($\text{L}\beta$), and 11.28 keV ($\text{L}\gamma$) for tungsten, along with an oxygen peak at 0.52 keV. The relative intensities of these peaks provided insights into the stoichiometry and elemental distribution of the synthesized nanoparticles.

3. Fourier Transform Infrared Spectroscopy (FTIR)

Fourier Transform Infrared Spectroscopy (FTIR) was employed to investigate the chemical bonding within pure TiO_2 , pure WO_3 , and TiO_2/WO_3 nanocomposites (1:1 and 2:1 ratios). FTIR spectra were recorded in the range of $500\text{--}4000\text{ cm}^{-1}$ (Figure 4.2). The fingerprint region ($600\text{--}1500\text{ cm}^{-1}$) was particularly informative for identifying metal-oxide bonds. Characteristic Ti-O and Ti-O-Ti stretching vibrations were observed between $400\text{--}800\text{ cm}^{-1}$, while W-O stretching vibrations appeared between $600\text{--}900\text{ cm}^{-1}$. Notably, absorption peaks at 516.79 cm^{-1} , 551.65 cm^{-1} , and 733.65 cm^{-1} corresponded to O-Ti-O vibrations, while peaks at 589.69 cm^{-1} , 755.58 cm^{-1} , and 802.4 cm^{-1} were associated with W-O bonds. An additional peak at 1064.88 cm^{-1} indicated the presence of oxide groups, confirming the successful formation of TiO_2 , WO_3 , and their nanocomposites.

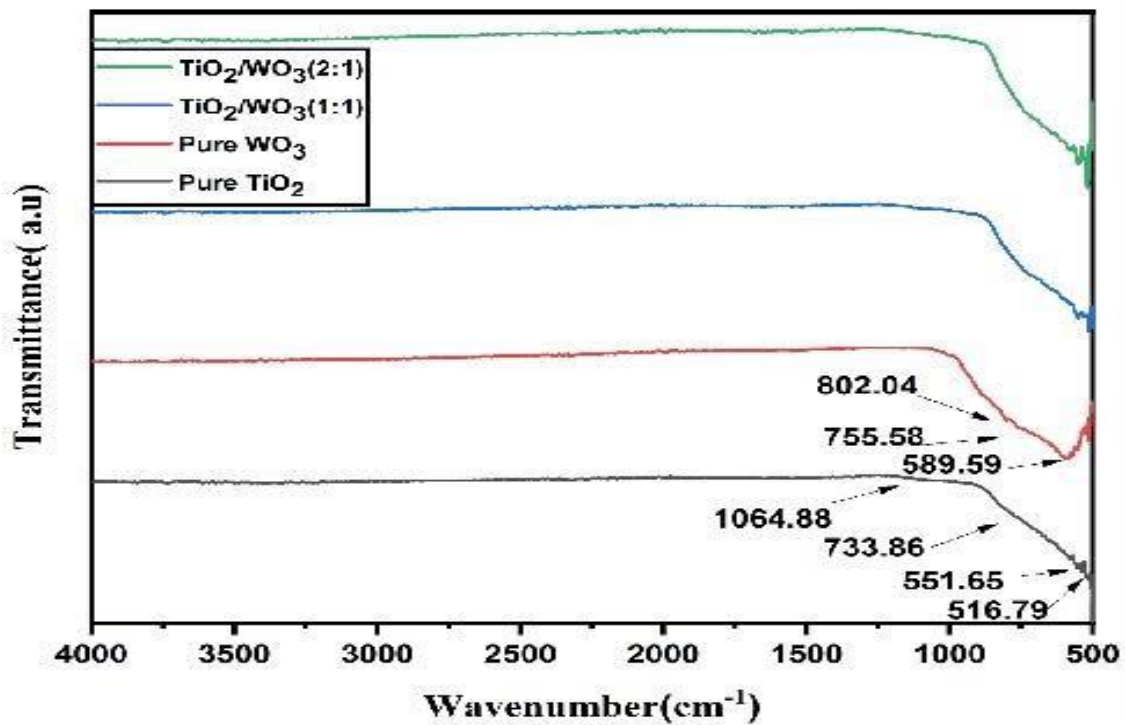
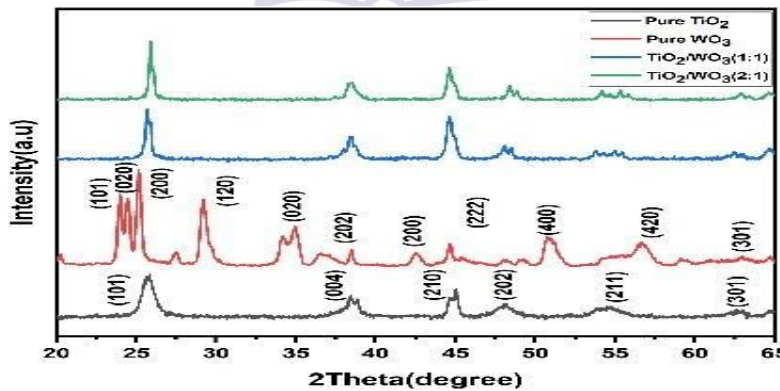


Figure 4.7: FTIR graph of TiO₂, WO₃, TiO₂ /WO₃ (1:1) & TiO₂ /WO₃ (2 :1)

Figure 4.8: XRD Pattern of pure TiO₂, pure WO₃, TiO₂ /WO₃ (1:1) & TiO₂ /(2 :1)



4. X-ray Diffraction Analysis

Materials synthesized using green synthesis techniques involved the utilization of X-ray diffraction (XRD) analysis. This analytical method was employed to ascertain phase identification and crystalline structure, and it also allowed for the calculation of the average crystallite size of the samples. For a comprehensive examination, XRD data for all the samples, including pure TiO₂ and pure WO₃

nanoparticles and WO₃/TiO₂ nanocomposites with varying ratios 1:1 & 2:1, were analyzed to determine parameters such as unit cell properties, lattice constants, and unit cell volume. Figure 4.1 illustrates the XRD spectra for pure TiO₂ NPs. The size of nanoparticles can be calculated with the help of the Debye-Scherrer formula.

$$D = (K \lambda) / (\beta \cos \theta)$$

Particle sizes smaller than 60 nm could be determined using the Debye-Scherrer equation.

- Crystalline size (D), where D is the particle's size and $D = K\lambda/\beta \cos \theta$. $K=0.94$ is referred to as Scherrer's constant.
- The wavelength of an X-ray is λ (1.54178Å).
- β is the full width at half maximum (FWHM) of the diffraction peak in radians.

XRD analysis was performed to find the crystallite size and phase impurities in the synthesized nanomaterial in the 2θ range of 20° - 65° . The observed XRD peaks for pure TiO₂ NPs are indexed at (101), (004), (210), (202), (211), and (311), which give a monoclinic crystal structure.

The observed XRD peaks for pure WO₃ NPs are indexed at (101), (020), (200), (120), (020),(202), (200), (222), (404), (420), and (301) which give monoclinic crystal structure. In nanocomposites, both TiO₂ and WO₃ peaks are parents, which shows the successful synthesis of TiO₂/WO₃ Nanocomposites. No extra peaks have been observed, indicating the formation of pure and their composite nanostructures. The average crystallite sizes of the pure TiO₂, WO₃, TiO₂/WO₃ (1:1), and TiO₂:WO₃ (2:1) are 41nm, 51nm, 48nm, and 57nm, respectively.

5. UV-Visible Spectroscopy Analysis

Ultraviolet-Visible (UV-Vis) spectroscopy is an essential analytical technique used to measure the

absorption and transmission of electromagnetic radiation by molecules, atoms, and electrons within the ultraviolet and visible light ranges (Quevedo et al., 2021). In this study, UV-Vis spectra were recorded over the wavelength range of 200–800 nm to investigate the optical properties of pure TiO₂, pure WO₃, and TiO₂/WO₃ nanocomposites (1:1 and 2:1 ratios).

Figure 4.9 presents the UV-Vis absorption spectra of the synthesized materials. The x-axis represents the wavelength (nm), while the y-axis indicates the absorbance. Pure TiO₂ nanoparticles exhibited a strong absorption peak at 259.06 nm, and pure WO₃ nanoparticles showed a peak at 534.81 nm. For the nanocomposites, absorption peaks were observed at 415.45 nm for TiO₂/WO₃ (2:1) and 415.02 nm for TiO₂/WO₃ (1:1), indicating a shift in the absorption edge due to composite formation.

The optical band gap energies were determined using the Tauc plot method, where the x-axis represents the photon energy (eV) and the y-axis corresponds to $(\alpha h\nu)^2$ for direct band gap transitions. The calculated band gaps were 3.01 eV for TiO₂, 2.92 eV for WO₃, 2.81 eV for TiO₂/WO₃ (2:1), and 2.49 eV for TiO₂/WO₃ (1:1). The observed reduction in band gap for the nanocomposites suggests enhanced light absorption in the visible region, beneficial for photocatalytic applications.

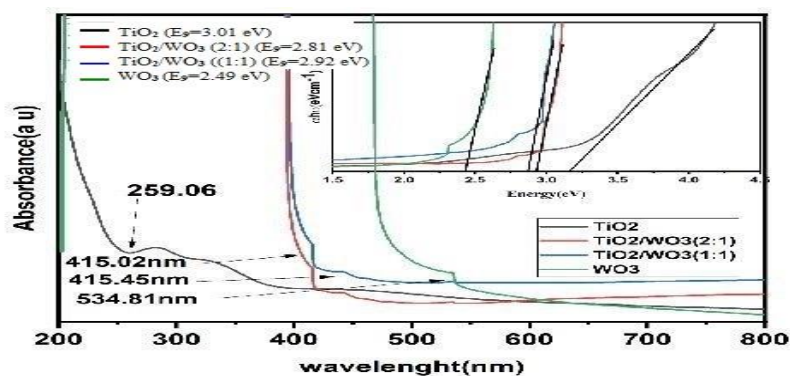


Figure 4.9 UV Graph of bandgap of pure TiO₂, pure WO₃, TiO₂ /WO₃ (1:1) & TiO₂ /WO₃ (2 :1)

6. Photocatalytic Activity

Photocatalytic activity refers to a photocatalyst's ability to initiate redox reactions under light exposure, crucially dependent on the semiconductor's band

structure. Upon sunlight irradiation, electrons are excited from the valence band to the conduction band, forming electron-hole pairs. These species drive oxidation and reduction reactions, generating

reactive radicals such as hydroxyl ($\bullet\text{OH}$) and superoxide ($\text{O}_2 \bullet^-$), which degrade organic pollutants into simpler molecules like CO_2 and H_2O .

In this study, the photocatalytic performance of TiO_2 , WO_3 , and TiO_2/WO_3 nanocomposites (ratios 1:1 and 2:1) synthesized via green methods was evaluated using methylene blue (MB) dye as a model pollutant. A 0.01 mg solution of MB was prepared in 500 mL of

distilled water, to which the photocatalyst was added. The mixture was exposed to natural sunlight between 10 AM and 2 PM, with continuous stirring to ensure uniform dispersion. Samples were collected at

intervals of 20, 40, 60, and 80 minutes and analyzed by UV-Vis spectrophotometry at 664 nm to monitor the degradation process.

The results showed a gradual decrease in the MB absorption peak from an initial 659.13 nm, indicating progressive degradation. The TiO_2/WO_3 (1:1) nanocomposite demonstrated superior photocatalytic efficiency compared to pure TiO_2 and WO_3 . The study confirms that the synthesized photocatalysts are effective for the breakdown of organic dyes, highlighting their potential application in environmental remediation.

Figure 4.10: Photocatalytic activity of TiO_2 .

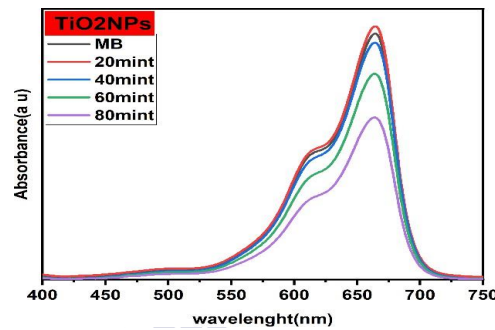
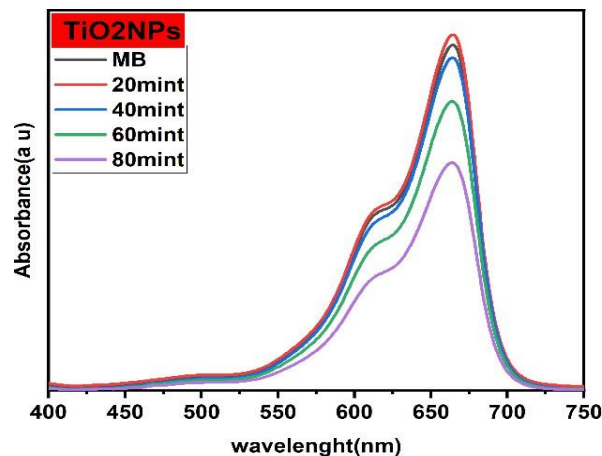


Figure 4.11: Photocatalytic activity of TiO_2



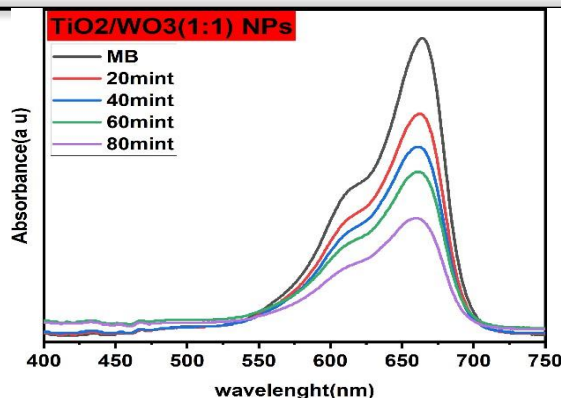


Figure 4.12: Photocatalytic activity of $\text{TiO}_2/\text{WO}_3(1:1)$.

IV. Conclusion

This study successfully demonstrated the green synthesis of pure TiO_2 , pure WO_3 , and TiO_2/WO_3 nanocomposites (ratios 2:1 and 1:1) using lemongrass (*Cymbopogon flexuosus*) leaf extract as an eco-friendly reducing and stabilizing agent. Comprehensive structural, morphological, chemical, and optical characterizations were performed using SEM, EDX, FTIR, XRD, and UV-Visible spectroscopy.

SEM and EDX analyses confirmed the uniform particle morphology and high purity of the synthesized nanomaterials. FTIR spectra verified the formation of Ti-O and W-O bonding, indicating the successful synthesis of individual oxides and their composites without unwanted functional groups. XRD analysis revealed well-defined crystalline structures, with average crystallite sizes of approximately 41 nm (TiO_2), 51 nm (WO_3), and 48–57 nm for the nanocomposites. UV-Vis spectroscopy and Tauc plot analysis showed a progressive reduction in band gap energy from 3.01 eV (TiO_2) to 2.49 eV (TiO_2/WO_3 1:1), enhancing visible-light absorption. Among the synthesized samples, the TiO_2/WO_3 (1:1) nanocomposite exhibited the highest photocatalytic performance, effectively degrading methylene blue dye under solar irradiation. These results underscore the potential of green-synthesized TiO_2/WO_3 nanocomposites as efficient and sustainable photocatalysts for environmental remediation applications.

References

- Sim & Wong Falara, P. P., Antoniadou, M., Zourou, A., Sakellis, E., & Kordatos, K. V. (2024). Carbon Dot- Titanium Dioxide (CD/ TiO_2) Nanocomposites: Reusable Photocatalyst for Sustainable H_2 Production via Photoreforming of Green Organic Compounds. *Coatings*, 14(1). <https://doi.org/10.3390/coatings14010131>
- Eychmüller, A. (2000). Structure and photophysics of semiconductor nanocrystals. *The Journal of Physical Chemistry B*, 104 (28), 6514–6528. <https://doi.org/10.1021/jp9943676>
- Edelstein, A. S., & Cammarata, R. C. (1998). *Nanomaterials: Synthesis, properties and applications*. Institute of Physics Publishing.
- Sim, L. C., & Wong, W. Y. (2021). Applications of nanotechnology in industry and medicine: A review. *Nanomaterials Today*, 35, 100978.
- Zhou, Y., Li, Y., Wang, X., & Zhang, M. (2011). Nanotechnology in environmental protection. *Journal of Environmental Sciences*, 23 (1), 1–10.
- Kiyamov, A., Mamedov, R., & Kadirova, J. (2020). Classification of nanoparticles based on chemical composition. *Journal of Nanomaterials Research*, 12 (3), 121–130.
- Khan, M. A., Shaik, M. R., & Adil, S. F. (2019). Nanoparticles: Types, classification, and applications. *Materials Today: Proceedings*, 18, 2143–2150.

- Jeon, S. J., & Baek, Y. W. (2010). Metal oxide nanoparticles and their applications in clean energy. *Korean Journal of Chemical Engineering*, 27 (6), 1782-1792.
- Siddiqui, M. N., Redhwi, H. H., & Majeed, M. I. (2020). Recent advances in nanomaterials and their impact on water treatment. *Environmental Nanotechnology, Monitoring & Management*, 14, 100346.
- Saleh, T. A., & Elkord, E. (2020). Review on applications of nanomaterials in environmental catalysis and water purification. *Journal of Environmental Chemical Engineering*, 8 (4), 104303.
- Gong, J., Zhou, M., & Guo, X. (2021). Inorganic nanomaterials for energy applications: A review. *Renewable and Sustainable Energy Reviews*, 135, 110251.
- Fujishima, A., Rao, T. N., & Tryk, D. A. (2000). Titanium dioxide photocatalysis. *Journal of Photochemistry and Photobiology C: Photochemistry Reviews*, 1(1), 1-21.
- Chen, X., & Mao, S. S. (2007). Titanium dioxide nanomaterials: Synthesis, properties, modifications, and applications. *Chemical Reviews*, 107(7), 2891-2959.
- Nosaka, Y., & Nosaka, A. Y. (2016). Understanding hydroxyl radical generation in photocatalysis. *ACS Energy Letters*, 1(2), 356-359.
- Kalathil, S., Khan, M. M., & Lee, J. (2013). Enhanced visible-light activity of TiO_2 through heterostructure formation. *Journal of Materials Chemistry A*, 1(21), 6135-6141.
- Hariharan, C., Ramesh, R., & Subramaniam, B. (2019). Visible-light-driven photocatalytic activity of WO_3 nanomaterials. *Materials Science in Semiconductor Processing*, 91, 215-223.
- Sánchez Martínez, D., Fernández Hevia, D., & González Alonso, D. (2011). Bandgap engineering in tungsten oxide thin films. *Thin Solid Films*, 519(17), 5776-5781.
- Salje, E. K. H., Aktas, O., Carpenter, M. A., Laguta, V. V., & Scott, J. F. (1997). Electron-hole dynamics in semiconductor heterostructures. *Journal of Applied Physics*, 82(3), 1415-1422.
- Han, C., Wang, Y., & Yu, J. (2021). Constructing TiO_2/WO_3 heterostructures for enhanced photocatalytic performance. *Applied Catalysis B: Environmental*, 285, 119838.
- Nguyen, V. H., Le, T. H., & Pham, T. T. (2018). Green synthesis of nanoparticles using plant extracts: A review. *Green Chemistry Letters and Reviews*, 11(4), 474-502.
- Parveen, K., Banse, V., & Ledwani, L. (2016). Green synthesis of nanoparticles: Their advantages and disadvantages. *Materials Science for Energy Technologies*, 1(1), 13-24.
- Srivastava, A. K. (2022). Lemongrass phytochemicals in nanoparticle synthesis: A green approach. *Journal of Green Chemistry and Sustainability*, 6(2), 89-97.
- Sahoo, D. P., & Goswami, M. (2024). Photocatalytic degradation of dyes using metal oxide nanocomposites. *Journal of Environmental Chemical Engineering*, 12(1), 108776.
- Goutam, S. P., Saxena, G., Roy, D., Yadav, A. K., & Bharagava, R. N. (2020). Role of metal oxide nanocomposites in wastewater treatment. *Environmental Nanotechnology, Monitoring & Management*, 13, 100284.